Chinese Journal of Aeronautics, (2015),28(1): 294–304

Chinese Society of Aeronautics and Astronautics
& Beihang University

Chinese Journal of Aeronautics

cja@buaa.edu.cn
www.sciencedirect.com

Fuzzy robust nonlinear control approach for electro-hydraulic flight motion simulator

Han Songshan, Jiao Zongxia *, Wang Chengwen, Shang Yaoxing

School of Automation Science and Electrical Engineering, Beihang University, Beijing 100191, China

Received 18 December 2013; revised 14 August 2014; accepted 28 September 2014
Available online 27 December 2014

KEYWORDS

Hydraulic control;
Flight simulation;
Fuzzy logic systems;
Nonlinear robust control;
Parametric uncertainties;
Uncertain nonlinearities

Abstract A fuzzy robust nonlinear controller for hydraulic rotary actuators in flight motion simulators is proposed. Compared with other three-order models of hydraulic rotary actuators, the proposed controller based on first-order nonlinear model is more easily applied in practice, whose control law is relatively simple. It not only does not need high-order derivative of desired command, but also does not require the feedback signals of velocity, acceleration and jerk of hydraulic rotary actuators. Another advantage is that it does not rely on any information of friction, inertia force and external disturbing force/torque, which are always difficult to resolve in flight motion simulators. Due to the special composite vane seals of rectangular cross-section and goalpost shape used in hydraulic rotary actuators, the leakage model is more complicated than that of traditional linear hydraulic cylinders. Adaptive multi-input single-output (MISO) fuzzy compensators are introduced to estimate nonlinear uncertain functions about leakage and bulk modulus. Meanwhile, the decomposition of the uncertainties is used to reduce the total number of fuzzy rules. Different from other adaptive fuzzy compensators, a discontinuous projection mapping is employed to guarantee the estimation process to be bounded. Furthermore, with a sufficient number of fuzzy rules, the controller theoretically can guarantee asymptotic tracking performance in the presence of the above uncertainties, which is very important for high-accuracy tracking control of flight motion simulators. Comparative experimental results demonstrate the effectiveness of the proposed algorithm, which can guarantee transient performance and better final accurate tracking in the presence of uncertain nonlinearities and parametric uncertainties.

1. Introduction

Hydraulic flight motion simulator (HFMS) has been widely used in hardware-in-the-loop simulation of various aircraft to verify performance indices of sensors, inertial navigation systems and flight control systems. It possesses many advantages including greater power-to-weight ratio, faster response time, larger force/torques output, higher stiffness and less electromagnetic interference compared with the corresponding

* Corresponding author. Tel.: +86 10 82338938.
E-mail address: zxjiao@buaa.edu.cn (Z. Jiao).

Peer review under responsibility of Editorial Committee of CJA.

Production and hosting by Elsevier

http://dx.doi.org/10.1016/j.cja.2014.12.025
1000-9361 © 2015 Production and hosting by Elsevier Ltd. on behalf of CSAA & BUAA.

electrical simulator.[1–3] As the typical hydraulic position/angle servo system, hydraulic rotary actuators in HFMS are highly nonlinear, including the nonlinear pressure-flow characteristics of servo valve, nonlinear friction, nonlinear dynamics of pressure, etc.[4,5] Aside from the above nonlinear nature of hydraulic dynamics, HFMS also has a large extent of uncertainties. The uncertainties can be classified into two categories: parametric uncertainties and uncertain nonlinearities.[6] Parametric uncertainties include the large change of payload and the variations in the hydraulic parameters (e.g. bulk modulus and leakage coefficient) due to the change of temperature and component wear. The other category is called uncertain nonlinearities which cannot be modeled exactly, such as nonlinear friction, unstructured leakage and external disturbances. How to deal with these uncertainties, improve the transient performance and guarantee steady-state accuracy, is a key issue in HFMS.

Lots of hydraulic controllers were designed by linear methods.[7–9] However, with increasing high tracking performance requirements in modern industrials, it is hard for linear controllers to achieve higher performance if a working point or the system properties change drastically in hydraulic systems. Vossoughi and Donath[10] developed feedback linearization techniques in electro-hydraulic control systems. Alleyne and Hedrick[11] applied the nonlinear adaptive control to solve parametric uncertainties of hydraulic cylinder. Yue et al.[12] developed robust adaptive control with state observers in hydraulic simulator. The direct adaptive robust control technique proposed by Yao et al.[13] was applied to precision motion control of single-rod actuators. To achieve better online parameter estimation properties to assist in secondary purposes such as fault detection and health monitoring, an indirect adaptive robust control design has recently been proposed.[14–16]

But most aforementioned adaptive controllers based on feedback linearization techniques largely focus on the structured uncertainties, or are restricted to unknown linear parameters. If there exists the unstructured nonlinear uncertainties, tracking precision will be affected due to incomplete compensation unless using switching functions or high feedback error gain. Therefore, unstructured uncertainties in hydraulic systems are the main obstacles to develop high-accuracy tracking control in HFMS. Fuzzy logic systems, radial basis function neural networks or feed-forward neural networks have been proved to be particularly powerful tools for solving uncertain nonlinear problems due to their universal approximation capability.[17–21]

Lots of fuzzy controller are PID-like controllers based on a nonlinear function of the errors, change of errors or acceleration errors, which rely on the trial and error method or a priori expert knowledge of the characteristic of the hydraulic actuators and lack enough adaptability.[22,23] The neuro-fuzzy controller tuned by the gradient-descent method was employed to get the actuator inverse-model, which did not contain stability analysis.[24] A sliding mode control scheme based on fuzzy cerebellar model articulation controller was proposed for the control of electro-hydraulic position system, whose adaptive law was derived based on Lyapunov method. However, the acceleration signal and third order derivative of desired signal must be known in its sliding mode control.[25] The adaptive fuzzy controller was introduced to approach the equivalent control of sliding mode control based on a linearized model of electro-hydraulic system and was verified by simulation. However, it must require the signals of acceleration and the derivative of acceleration as input variables to the fuzzy controller, which are always noisy and are not recommended in practice.[26,27] Most of the above adaptive fuzzy controller adopted the error equations of velocity, acceleration and jerk, which were required in the design procedure of the back-stepping control or sliding mode variable structure control. In this paper, a simple robust nonlinear controller based on adaptive multi-input single-output (MISO) fuzzy compensators are synthesized to deal with uncertain nonlinearities and parametric uncertainties in hydraulic rotary actuator of HFMS, which does not need acceleration, jerk and high-order derivative of desired signal.

A method to reduce the number of total fuzzy rules through the decomposition of uncertainty function is also proposed. Uncertainty functions are decomposed into two parts, uncertainty related with leakage and uncertainty related with fluid elastic. Due to the special composite vane seals of rectangular cross-section and goalpost shape used in hydraulic rotary actuators of HFMS, the leakage model is more complicated than that of traditional linear hydraulic cylinders. So different from traditional leakage model proportional to the load-pressure P_L, the leakage model in this paper is considered as the nonlinear function related to P_L and the output angle x_1 of motor. The flow of fluid elastic compression is also taken as the nonlinear function related to load-pressure's derivative $\dot{P}_L$ and x_1. So two MISO fuzzy logic compensators (FLCs) are adopted to estimate the above nonlinear functions respectively. Different from other adaptive fuzzy compensators,[24–30] in order to guarantee that the estimation process is bounded and the system is stable, a discontinuous projection mapping is employed in adaptive fuzzy compensators. So the proposed controller accounts for not only the structured uncertainties (i.e. parametric uncertainties), but also the unstructured uncertainties (i.e. unstructured items of leakage and fluid elastic compression). Furthermore, the controller can theoretically achieve a guaranteed transient performance and final tracking accuracy in the presence of the above uncertainties, which is very important for high-accuracy tracking control of HFMS. Finally, comparative experimental results are presented for the motion control of a hydraulic rotary actuator to verify the effectiveness of the proposed controller.

2. System description and problem formulation

The flight motion simulator in Fig. 1 is configured with an orthogonal outer axis frame (yaw), a middle axis frame (pitch) which is horizontal to the outer axis, and an inner axis frame (roll) supported by the middle axis frame and a base. The inner axis has limited angular freedom and is driven by a hydraulic rotary actuator that is fixed onto the middle frame to rotate about the roll axis. A hard-anodized aluminum tabletop on the roll axis serves as the payload mounting surface. The outer axis frame with limited angular motion rotates around a vertical yaw axis and is driven by a hydraulic rotary actuator located inside the base. The middle axis frame with limited angular motion moves around a horizontal pitch axis and is driven by another hydraulic rotary actuator, which is fixed onto the outer frame. The hydraulic rotary actuator in HFMS is also described by Fig. 1, which consists of servo-valve, controller, hydraulic motor, load and angle encoder.

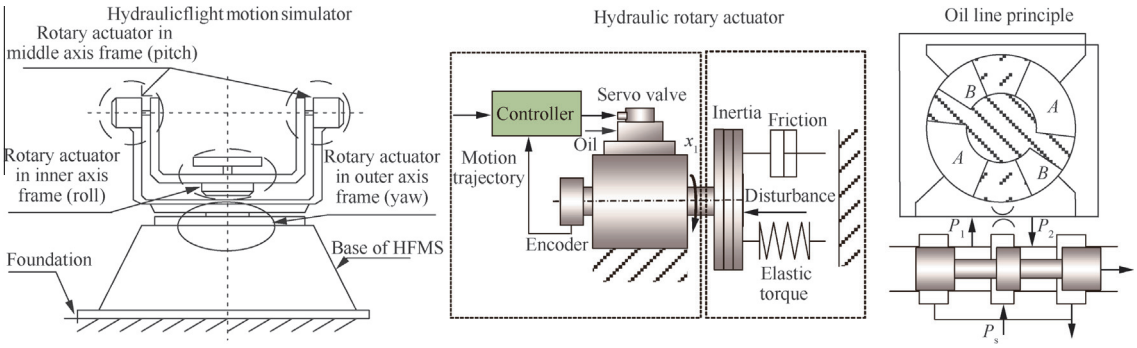

Fig. 1 Architecture and oil line principle of hydraulic rotary actuator in HFMS.

The flow continuity equation of hydraulic rotary actuator in HFMS is given in Ref. [5]

$$Q_{\mathrm{L}} = Q_{\mathrm{Motion}} + Q_{\mathrm{Leakage}} + Q_{\mathrm{Elastic}} \tag{1}$$

where Q_{L} is the flow of servo-valve, which can be seen as controlled flow; Q_{Motion} is the motion flow of hydraulic motor , which can be calculated by Eq. (2); Q_{Leakage} is the leakage flow of hydraulic motor; Q_{Elastic} is the fluid elasticity compression flow.

$$Q_{\mathrm{Motion}} = D_{\mathrm{L}}\dot{x}_1 \tag{2}$$

where D_{L} is the displacement of hydraulic motor and $\dot{x}_1$ is the angular velocity.

Assume that external leakage of motor is negligible. Then Q_{Leakage} can be given as

$$Q_{\mathrm{Leakage}} = C_{\mathrm{t}}P_{\mathrm{L}} - d_{\mathrm{L1}} \tag{3}$$

where C_{t} is the coefficient of the internal leakage of motor; P_{L} is the pressure difference between the two chambers of motor, P_1 and P_2, i.e. $P_{\mathrm{L}} = P_1 - P_2$; d_{L1} is an unknown nonlinear leakage function. Considering the special composite vane seals of rectangular cross section and goalpost shape used in hydraulic rotary actuators,[31] the internal leakage is more complicated than that of traditional linear hydraulic cylinders. So, in this paper, the internal leakage model of rotary actuators is considered as the nonlinear function related to P_{L} and the output angle x_1. For example, when the hydraulic rotary actuator is fixed at the middle location to avoid its movement in Ref. [32], the leakage flow model has been identified as

$$Q_{\mathrm{Leakage}} = c_1P_{\mathrm{L}}^2 + c_2P_{\mathrm{L}} + c_3 \tag{4}$$

where c_1, c_2 and c_3 are leakage coefficients identified by experiments.

Q_{Elastic} is given as

$$Q_{\mathrm{Elastic}} = \frac{V_{\mathrm{t}}}{4\beta_{\mathrm{e}}}\dot{P}_{\mathrm{L}} - d_{\mathrm{L2}} \tag{5}$$

where V_{t} is the total control volume; β_{e} is the effective bulk modulus; d_{L2} is an unknown nonlinear function, which is mostly influenced by the load-pressure's derivative $\dot{P}_{\mathrm{L}}$ and position x_1.

For simplification, assume that the servo valve is matched symmetrically with ideal zero opening and zero lapping; radial-clearance leakage of the valve's spool can be negligible, oil source pressure is stable and return pressure is zero. Based on these assumptions, the load flow equation given by Ref. [5] shows:

$$Q_{\mathrm{L}} = D_{\mathrm{L}}\dot{x}_1 + C_{\mathrm{t}}P_{\mathrm{L}} + \frac{V_{\mathrm{t}}}{4\beta_{\mathrm{e}}}\dot{P}_{\mathrm{L}} - D_{\mathrm{L}}d_{\mathrm{L}} \tag{6}$$

with $D_{\mathrm{L}}d_{\mathrm{L}} = d_{\mathrm{L1}} + d_{\mathrm{L2}}$.

Rewriting Eq. (6) yields that

$$\dot{x}_1 = \alpha Q_{\mathrm{L}} - \theta_1P_{\mathrm{L}} - \theta_2\dot{P}_{\mathrm{L}} + d_{\mathrm{L}} \tag{7}$$

where $\alpha = 1/D_{\mathrm{L}}$, $\theta_1 = C_{\mathrm{t}}/D_{\mathrm{L}}$ and $\theta_2 = V_{\mathrm{t}}/(4\beta_{\mathrm{e}}D_{\mathrm{L}})$.

The load flow Q_{L} governed by the spool displacement given by Ref. [5] shows:

$$Q_{\mathrm{L}} = C_{\mathrm{d}}\omega x_{\mathrm{v}}\sqrt{P_{\mathrm{s}} - \mathrm{sgn}(x_{\mathrm{v}})P_{\mathrm{L}}/\rho} \tag{8}$$

where C_{d} is the flow coefficient of valve; ω is the area gradient of valve; ρ is the oil's density; x_{v} is the spool displacement; and P_{s} is the oil source pressure. sgn (*) denotes the discontinuous sign function and it is defined as

$$\mathrm{sgn}(*) = \begin{cases} 1 & \text{If } * > 0 \\ 0 & \text{If } * = 0 \\ -1 & \text{If } * < 0 \end{cases} \tag{9}$$

The effect of servo-valve dynamics has been included in some literature. However, additional sensors are required to obtain the spool position and it significantly increases the complexities in real-time controller implementation. Therefore, many researchers neglect servo-valve dynamics.[14,15,32–34] Considering that the spool dynamic of servo valve used in this paper is much higher than that of HFMS, assume that the control applied to the servo valve is directly proportional to the spool position, i.e. $x_{\mathrm{v}} = k_{x\mathrm{v}}u$, where $k_{x\mathrm{v}}$ is the valve gain and u is the control input.

Although we do not have the accurate values of the unknown parameter set $\boldsymbol{\theta}$, for most applications, the extents of the parametric uncertainties and uncertain nonlinearities are known. Thus the following practical assumption is made.

Assumption 1. Parametric uncertainties satisfy

$$\boldsymbol{\theta} \in \boldsymbol{\Omega}_{\boldsymbol{\theta}} \triangleq \{\boldsymbol{\theta} : \boldsymbol{\theta}_{\min} \leqslant \boldsymbol{\theta} \leqslant \boldsymbol{\theta}_{\max}\} \tag{10}$$

where $\boldsymbol{\theta} = [\theta_1, \theta_2]^{\mathrm{T}}$; $\boldsymbol{\theta}_{\min} = [\theta_{1\min}, \theta_{2\min}]^{\mathrm{T}}$ and $\boldsymbol{\theta}_{\max} = [\theta_{1\max}, \theta_{2\max}]^{\mathrm{T}}$ are known lower and upper bound vectors of $\boldsymbol{\theta}$; $\boldsymbol{\Omega}_{\boldsymbol{\theta}}$ is the known bounded set of $\boldsymbol{\theta}$. Uncertain nonlinearities d_{L1}, d_{L2} and d_L satisfy

$$\begin{cases} |d_{\mathrm{L1}}| \leqslant \delta_1(t) \\ |d_{\mathrm{L2}}| \leqslant \delta_2(t) \\ |d_{\mathrm{L}}| \leqslant \delta_{\mathrm{L}}(t) \end{cases} \tag{11}$$

where $\delta_1(t)$, $\delta_2(t)$ and $\delta_L(t)$ are known bound functions.

Given the desired angle reference $x_{1d}(t)$, our aim is to synthesize a control input u such that angle input x_1 tracks $x_{1d}(t)$ as closely as possible in spite of parameter uncertainties or unstructured nonlinear uncertainties in HFMS.

3. Design of fuzzy nonlinear robust controller

3.1. Robust controller design

Define the angle tracking error as e_1

$$e_1 = x_1 - x_{1d} \tag{12}$$

Its time derivative of e_1 is given as

$$\dot{e}_1 = \dot{x}_1 - \dot{x}_{1d} \tag{13}$$

Substituting Eq. (7) into Eq. (13) yields that

$$\dot{e}_1 = \alpha Q_L - \theta_1 P_L - \theta_2 \dot{P}_L + d_L - \dot{x}_{1d} \tag{14}$$

It is not easy to know the accurate parameters in the presence of uncertain nonlinearities. So define

$$\begin{cases} \theta_1 = \theta_{10} + \tilde{\theta}_1 \\ \theta_2 = \theta_{20} + \tilde{\theta}_2 \end{cases} \tag{15}$$

where θ_{10} and θ_{20} are nominal values; $\tilde{\theta}_1$ and $\tilde{\theta}_2$ present unknown values of θ_1 and θ_2, respectively.

Substituting Eq. (14) into Eq. (15) yields that

$$\dot{e}_1 = \alpha Q_L - \theta_{10} P_L - \theta_{20} \dot{P}_L - \tilde{\theta}_1 P_L - \tilde{\theta}_2 \dot{P}_L + d_L - \dot{x}_{1d} \tag{16}$$

Define Lyapunov function

$$V_1 = \frac{1}{2} e_1^2 \tag{17}$$

Its time derivative according to Eq. (16) is given as

$$\dot{V}_1 = e_1(\alpha Q_L - \theta_{10} P_L - \theta_{20} \dot{P}_L - \tilde{\theta}_1 P_L - \tilde{\theta}_2 \dot{P}_L + d_L - \dot{x}_{1d}) \tag{18}$$

Define

$$\boldsymbol{\varphi} = [P_L, \dot{P}_L]^T \tag{19}$$

Rewrite Eq. (18) according to Eq. (19):

$$\dot{V}_1 = e_1 \dot{e}_1 = e_1[\alpha Q_L - (\theta_{10} P_L + \theta_{20} \dot{P}_L + \dot{x}_{1d}) - (\tilde{\boldsymbol{\theta}}^T \boldsymbol{\varphi} - d_L)] \tag{20}$$

where $\tilde{\boldsymbol{\theta}} = [\tilde{\theta}_1, \ \tilde{\theta}_2]$ and $\tilde{\boldsymbol{\theta}}^T \boldsymbol{\varphi} = \tilde{\theta}_1 P_L + \tilde{\theta}_2 \dot{P}_L$. $\tilde{\boldsymbol{\theta}}^T \boldsymbol{\varphi} - d_L$ represents the uncertainties, which is the sum of parameter uncertainties $\tilde{\boldsymbol{\theta}}^T \boldsymbol{\varphi}$ and uncertain nonlinearities d_L.

If take Q_L as the control input in Eq. (20), tracking error e_1 is mainly affected by $\theta_{10} \dot{P}_L + \theta_{20} P_L + \dot{x}_{1d}$ and $\tilde{\boldsymbol{\theta}}^T \boldsymbol{\varphi} - d_L$. $\theta_{10} \dot{P}_L + \theta_{20} P_L + \dot{x}_{1d}$, which is exactly known, could be easily compensated. In this case, tracking error e_1 just depends upon the uncertainties $\tilde{\boldsymbol{\theta}}^T \boldsymbol{\varphi} - d_L$. So it can be concluded that parameter uncertainties $\tilde{\boldsymbol{\theta}}^T \boldsymbol{\varphi}$ and uncertain nonlinearities d_L will seriously affect tracking error e_1.

The traditional robust controllers to deal with the above uncertainties can be classified into two categories. The first one, like sliding surface controller, adopts switching function $k_s \mathrm{sgn}(e_1)$, which may cause chatting phenomenon; the second one uses strong error feedback term $k_s e_1$, which sacrifices asymptotic output tracking in theory. In the above two robust controllers, the larger uncertainties is, the larger feedback gain k_s is. High tracking accuracy can only be obtained with large feedback gain k_s, which is not recommended in practice. In this paper, adaptive MISO FLCs are introduced to deal with the above uncertainties in HFMS.

3.2. Design of adaptive fuzzy compensators

Parametric uncertainties $\tilde{\boldsymbol{\theta}}^T \boldsymbol{\varphi}$ and uncertain nonlinearities d_L compose all uncertainty stems from Eq. (18), which are mostly influenced by P_L, $\dot{P}_L$ and x_1. Therefore, P_L, $\dot{P}_L$ and x_1 can be adopted as the input variables in MISO FLC to compensate all uncertainty stems. However, if select k fuzzy labels on each input variable of the FLC, the fuzzy compensator needs k^3 fuzzy rules, where k^3 is the number of rules in the antecedent part of the FLC. To reduce the number of fuzzy rules, all uncertainty stems f_u in this paper will be divided into two parts:

$$\underbrace{(\tilde{\boldsymbol{\theta}}^T \boldsymbol{\varphi} - d_L)}_{f_u(P_L, \dot{P}_L, x_1, t)} = \underbrace{(\tilde{\theta}_1 P_L - d_{L1}/D_L)}_{g(P_L, x_1, t)} + \underbrace{(\tilde{\theta}_2 \dot{P}_L - d_{L2}/D_L)}_{h(\dot{P}_L, x_1, t)} \tag{21}$$

where $g(P_L, x_1, t)$ is uncertainty stems from $Q_{Leakage}$, which is mostly influenced by P_L and x_1;$h(\dot{P}_L, x_1, t)$ is uncertainty stems from $Q_{Elastic}$, which is mostly influenced by $\dot{P}_L$ and x_1.

So we can use two FLCs $\hat{g}$ and $\hat{h}$ to compensate for the above uncertainties respectively. In this case, the number of fuzzy rules decline from k^3 to $2k^2$, which is welcome in engineering practices.

Then the FLCs can be written as[32]

$$\begin{cases} \hat{g}(P_L, x_1 | \boldsymbol{\Theta}_g) = \dfrac{\sum_{l_1=1}^{k} \sum_{l_2=1}^{k} \left(\bar{y}_g^{l_1 l_2} \mu_{A_1^{l_1}}(P_L) \mu_{A_2^{l_2}}(x_1) \right)}{\sum_{l_1=1}^{k} \sum_{l_2=1}^{k} \left(\mu_{A_1^{l_1}}(P_L) \mu_{A_2^{l_2}}(x_1) \right)} = \boldsymbol{\Theta}_g^T \boldsymbol{\xi}_g(P_L, x_1, t) \\ \hat{h}(\dot{P}_L, x_1 | \boldsymbol{\Theta}_h) = \dfrac{\sum_{l_2=1}^{k} \sum_{l_3=1}^{k} \left(\bar{y}_h^{l_2 l_3} \mu_{A_2^{l_2}}(x_1) \mu_{A_3^{l_3}}(\dot{P}_L) \right)}{\sum_{l_2=1}^{k} \sum_{l_3=1}^{k} \left(\mu_{A_2^{l_2}}(x_1) \mu_{A_3^{l_3}}(\dot{P}_L) \right)} = \boldsymbol{\Theta}_h^T \boldsymbol{\xi}_h(\dot{P}_L, x_1, t) \end{cases} \tag{22}$$

where

$$\boldsymbol{\Theta}_g = [\bar{y}_g^1, \bar{y}_g^2, \ldots, \bar{y}_g^{k^2}]^T, \quad \boldsymbol{\Theta}_h = [\bar{y}_h^1, \bar{y}_h^2, \ \ldots \ , \bar{y}_h^{k^2}]^T,$$

$$\boldsymbol{\xi}_g = [\xi_g^1, \xi_g^2, \ldots, \xi_g^{k^2}]^T, \quad \boldsymbol{\xi}_h = [\xi_h^1, \xi_h^2, \ldots, \xi_h^{k^2}]^T,$$

with

$$\begin{cases} \xi_g^i = \dfrac{\mu_{A_1^{l_1}}(P_L) \mu_{A_2^{l_2}}(x_1)}{\sum_{l_1=1}^{k} \sum_{l_2=1}^{k} \left(\mu_{A_1^{l_1}}(P_L) \mu_{A_2^{l_2}}(x_1) \right)} \\ \xi_h^i = \dfrac{\mu_{A_2^{l_2}}(x_1) \mu_{A_3^{l_3}}(\dot{P}_L)}{\sum_{l_2=1}^{k} \sum_{l_3=1}^{k} \left(\mu_{A_2^{l_2}}(x_1) \mu_{A_3^{l_3}}(\dot{P}_L) \right)} \end{cases} \quad (i = 1, 2, \ldots, k^2)$$

where $A_1^{l_1}$, $A_2^{l_2}$ and $A_3^{l_3}$ are fuzzy sets of P_L, $\dot{P}_L$ and x_1, respectively; $\mu_{A_1^{l_1}}(P_L)$, $\mu_{A_2^{l_2}}(x_1)$ and $\mu_{A_3^{l_3}}(\dot{P}_L)$ are membership functions of P_L, $\dot{P}_L$ and x_1, respectively.

Assume the column vectors of the optimal parameter $\boldsymbol{\Theta}_g^*$ and $\boldsymbol{\Theta}_h^*$ as

$$\begin{cases} \boldsymbol{\Theta}_g^* = \arg\min\limits_{\boldsymbol{\Theta}_g \in \boldsymbol{\Omega}_g} \left(\sup\limits_{P_L \in \Omega_{P_L}, x_1 \in \Omega_{x_1}} |\hat{g}(P_L, x_1|\boldsymbol{\Theta}_g) - g(P_L, x_1, t)| \right) \\ \quad \triangleq \left[\bar{y}_g^{1*}, \bar{y}_g^{2*}, \ldots, \bar{y}_g^{k^2*} \right]^{\mathrm{T}} \\ \boldsymbol{\Theta}_h^* = \arg\min\limits_{\boldsymbol{\Theta}_h \in \boldsymbol{\Omega}_h} \left(\sup\limits_{\dot{P}_L \in \Omega_{\dot{P}_L}, x_1 \in \Omega_{x_1}} |\hat{h}(\dot{P}_L, x_1|\boldsymbol{\Theta}_h) - h(\dot{P}_L, x_1, t)| \right) \\ \quad \triangleq [\bar{y}_h^{1*}, \bar{y}_h^{2*}, \ldots, \bar{y}_h^{k^2*}]^{\mathrm{T}} \end{cases} \tag{23}$$

where $\boldsymbol{\Omega}_g$, $\boldsymbol{\Omega}_h$, Ω_{P_L}, Ω_{x_1} and $\Omega_{\dot{P}_L}$ are sets of $\boldsymbol{\Theta}_g$, $\boldsymbol{\Theta}_h$, P_L, x_1 and $\dot{P}_L$, respectively.

The following assumption to be used in the next section is made.

Assumption 2. The column vectors of the optimal parameter $\boldsymbol{\Theta}_g^*$ and $\boldsymbol{\Theta}_h^*$ satisfy

$$\begin{cases} \boldsymbol{\Theta}_g^* \in \boldsymbol{\Omega}_g \triangleq \{\boldsymbol{\Theta}_g^* : \boldsymbol{\Omega}_{g\min} \leqslant \boldsymbol{\Theta}_g^* \leqslant \boldsymbol{\Omega}_{g\max}\} \\ \qquad \triangleq \bar{y}_{g\min}^i \leqslant \bar{y}_g^{i^*} \leqslant \bar{y}_{g\max}^i \\ \boldsymbol{\Theta}_h^* \in \boldsymbol{\Omega}_h \triangleq \{\boldsymbol{\Theta}_h^* : \boldsymbol{\Omega}_{h\min} \leqslant \boldsymbol{\Theta}_h^* \leqslant \boldsymbol{\Omega}_{h\max}\} \\ \qquad \triangleq \bar{y}_{h\min}^i \leqslant \bar{y}_h^{i^*} \leqslant \bar{y}_{h\max}^i \end{cases} \quad (i = 1, 2, \ldots, k^2) \tag{24}$$

where $\boldsymbol{\Omega}_{g\min} = [\bar{y}_{g\min}^1, \bar{y}_{g\min}^2, \ldots, \bar{y}_{g\min}^{k^2}]^{\mathrm{T}}$, $\boldsymbol{\Omega}_{g\max} = [\bar{y}_{g\max}^1, \bar{y}_{g\max}^2, \ldots, \bar{y}_{g\max}^{k^2}]^{\mathrm{T}}$, $\boldsymbol{\Omega}_{h\min} = [\bar{y}_{h\min}^1, \bar{y}_{h\min}^2, \ldots, \bar{y}_{h\min}^{k^2}]^{\mathrm{T}}$ and $\boldsymbol{\Omega}_{h\max} = [\bar{y}_{h\max}^1, \bar{y}_{h\max}^2, \ldots, \bar{y}_{h\max}^{k^2}]^{\mathrm{T}}$ are known.

3.3. Discontinuous projection mapping

Different from other adaptive fuzzy compensators,[24–29] the adaptive law with projection type is employed to avoid the unstable FLCs estimation:

$$\begin{cases} \dot{\boldsymbol{\Theta}}_j = \mathrm{Proj}_{\boldsymbol{\Theta}_j}(\gamma_j \boldsymbol{\tau}_j), \quad \boldsymbol{\Theta}_j(0) \in \boldsymbol{\Omega}_j \ (j = g, h) \\ \boldsymbol{\tau}_g = -e_1 \boldsymbol{\xi}_g(P_L, x_1) \\ \boldsymbol{\tau}_h = -e_1 \boldsymbol{\xi}_h(\dot{P}_L, x_1) \end{cases} \tag{25}$$

where γ_j is positive adaptation gain and $\boldsymbol{\tau}_j$ is adaptation function of $\boldsymbol{\Theta}_j$. The discontinuous projection mapping $\mathrm{Proj}_{\boldsymbol{\Theta}_j}(*_j)$ is defined by Ref. [13]

$$\mathrm{Proj}_{\boldsymbol{\Theta}_j}(*_i) = \begin{cases} 0 & \text{If } \bar{y}_j^i = \bar{y}_{j\max}^i \text{ and } *_i > 0 \\ 0 & \text{If } \bar{y}_j^i = \bar{y}_{j\min}^i \text{ and } *_i < 0 \\ *_i & \text{Otherwise} \end{cases} \tag{26}$$

In Eq. (26), $*_i$ represents the ith component of the vector $*$ and $\bar{y}_j^i$ is the ith component of the vector $\boldsymbol{\Theta}_j$. For any adaption function $\boldsymbol{\tau}_j$, the projection mapping used in Eq. (26) guarantees

$$\begin{cases} (P1)\boldsymbol{\Theta}_j \in \boldsymbol{\Omega}_j \triangleq \{\boldsymbol{\Theta}_j : \boldsymbol{\Omega}_{j\min} \leqslant \boldsymbol{\Theta}_j \leqslant \boldsymbol{\Omega}_{j\max}\} \\ \qquad \triangleq \bar{y}_{j\min}^i \leqslant \bar{y}_j^i \leqslant \bar{y}_{j\max}^i \\ (P2)\tilde{\boldsymbol{\Theta}}_j^{\mathrm{T}}(\gamma_j^{-1}\mathrm{Proj}_{\boldsymbol{\Theta}_j}(\gamma \boldsymbol{\tau}_j) - \boldsymbol{\tau}_j) \leqslant 0, \forall \boldsymbol{\tau}_j \end{cases} \tag{27}$$

where $\tilde{\boldsymbol{\Theta}}_j = \boldsymbol{\Theta}_j^* - \boldsymbol{\Theta}_j$ is the estimation error.

3.4. Fuzzy nonlinear robust control law

With the optimal parameter vectors of the FLCs in Eq. (23), the minimum approximation errors can be defined as

$$\begin{cases} w_g = g(P_L, x_1, t) - \hat{g}(P_L, x_1|\boldsymbol{\Theta}_g^*) \\ w_h = h(\dot{P}_L, x_1, t) - \hat{h}(\dot{P}_L, x_1|\boldsymbol{\Theta}_h^*) \end{cases} \tag{28}$$

with

$$\|w_g\| \leqslant W_g, \quad \|w_h\| \leqslant W_h$$

where W_g and W_h are positive parameters.

From Eqs. (23) and (28), we can get

$$\begin{cases} g(P_L, x_1, t) - \hat{g}(P_L, x_1|\boldsymbol{\Theta}_g) \\ \quad = \boldsymbol{\Theta}_g^{*\mathrm{T}} \boldsymbol{\xi}_g(P_L, x_1) + w_g - \boldsymbol{\Theta}_g^{\mathrm{T}} \boldsymbol{\xi}_g(P_L, x_1) \\ \quad = \tilde{\boldsymbol{\Theta}}_g^{\mathrm{T}} \boldsymbol{\xi}_g(P_L, x_1) + w_g \\ h(\dot{P}_L, x_1, t) - \hat{h}(\dot{P}_L, x_1|\boldsymbol{\Theta}_h) \\ \quad = \boldsymbol{\Theta}_h^{*\mathrm{T}} \boldsymbol{\xi}_h(\dot{P}_L, x_1) + w_h - \boldsymbol{\Theta}_h^{\mathrm{T}} \boldsymbol{\xi}_h(\dot{P}_L, x_1) \\ \quad = \tilde{\boldsymbol{\Theta}}_h^{\mathrm{T}} \boldsymbol{\xi}_h(\dot{P}_L, x_1) + w_h \end{cases} \tag{29}$$

Substituting Eqs. (21) and (29) into Eq. (20) yields that

$$\begin{aligned} \dot{V}_1 &= e_1(\alpha Q_L - \theta_{10} P_L - \theta_{20} \dot{P}_L - \dot{x}_{1d} - g(P_L, x_1, t) \\ &\quad - h(\dot{P}_L, x_1, t)) \\ &= e_1(\alpha Q_L - \theta_{10} P_L - \theta_{20} \dot{P}_L - \dot{x}_{1d} - \hat{g}(P_L, x_1|\boldsymbol{\Theta}_g) \\ &\quad - \tilde{\boldsymbol{\Theta}}_g^{\mathrm{T}} \boldsymbol{\xi}_g(P_L, x_1) - w_g - \hat{h}(\dot{P}_L, x_1|\boldsymbol{\Theta}_h) \\ &\quad - \tilde{\boldsymbol{\Theta}}_h^{\mathrm{T}} \boldsymbol{\xi}_h(\dot{P}_L, x_1) - w_h) \end{aligned} \tag{30}$$

If Q_L is treated as the control input, a desired flow can be synthesized to ensure that $\dot{V}_1$ is semi-negative definite, equivalently, to make the tracking error dynamic is stable. The desired flow consists of two parts:

$$Q_L = Q_{La} + Q_{Lr} \tag{31}$$

where

$$\begin{cases} Q_{La} = \frac{1}{\alpha}(\dot{x}_{1d} + \theta_{10} \dot{P}_L + \theta_{20} P_L + \hat{g}(P_L, x_1|\boldsymbol{\Theta}_g) + \hat{h}(\dot{P}_L, x_1|\boldsymbol{\Theta}_h)) \\ Q_{Lr} = Q_{Lr1} + Q_{Lr2} \end{cases}$$

with

$$\begin{cases} Q_{Lr1} = -\frac{1}{\alpha} k_1 e_1 \\ Q_{Lr2} = -\frac{1}{\alpha} k_s(P_L, \dot{P}_L, x_1) e_1 \end{cases}$$

where k_1 is a positive gain. Rewrite Eq. (30) according to Eq. (31):

$$\begin{aligned} \dot{V}_1 &= e_1[(\alpha Q_{La} - \dot{x}_{1d} - \theta_{10} P_L - \theta_{20} \dot{P}_L - \hat{g}(P_L, x_1|\boldsymbol{\Theta}_g) \\ &\quad - \hat{h}(\dot{P}_L, x_1|\boldsymbol{\Theta}_h)) + \alpha Q_{Lr1} + (\alpha Q_{Lr2} - \tilde{\boldsymbol{\Theta}}_g^{\mathrm{T}} \boldsymbol{\xi}_g(P_L, x_1) \\ &\quad - \tilde{\boldsymbol{\Theta}}_h^{\mathrm{T}} \boldsymbol{\xi}_h(\dot{P}_L, x_1) - w_g - w_h)] \end{aligned} \tag{32}$$

For the robust design, we make the robust term Q_{Lr2} be any function satisfying the following conditions:

$$e_1(\alpha Q_{Lr2} - \tilde{\boldsymbol{\Theta}}_g^{\mathrm{T}} \boldsymbol{\xi}_g(P_L, x_1) - \tilde{\boldsymbol{\Theta}}_h^{\mathrm{T}} \boldsymbol{\xi}_h(\dot{P}_L, x_1) - w_g - w_h) \leqslant \varepsilon \tag{33}$$

$$\alpha e_1 Q_{Lr2} \leqslant 0 \tag{34}$$

where ε is a positive design parameter which can be arbitrarily small and represents the given robust accuracy.

Many methods can be used to choose a robust term Q_{Lr2} satisfying Eqs. (33) and (34). Here an example is given as follows:

Let h_1 be any smooth function satisfying

$$h_1 \geqslant \|\boldsymbol{\Theta}_{g\mathrm{M}}\|^2\|\boldsymbol{\xi}_g(P_\mathrm{L},x_1)\|^2+\|\boldsymbol{\Theta}_{h\mathrm{M}}\|^2\|\boldsymbol{\xi}_h(\dot{P}_\mathrm{L},x_1)\|^2+W_g+W_h \tag{35}$$

where $\boldsymbol{\Theta}_{g\mathrm{M}}=\boldsymbol{\Omega}_{g\max}-\boldsymbol{\Omega}_{g\min},\boldsymbol{\Theta}_{h\mathrm{M}}=\boldsymbol{\Omega}_{h\max}-\boldsymbol{\Omega}_{h\min};\quad\|\cdot\|$ denotes the 2-norm of a matrix or a vector. Then Q_{Lr2} can be chosen as

$$Q_{Lr2}=-\frac{1}{\alpha}k_s(\dot{P}_\mathrm{L},P_\mathrm{L},x_1)e_1\triangleq-\frac{1}{\alpha}\frac{h_1}{4\theta_{1\min}\varepsilon}e_1 \tag{36}$$

3.5. Performance and stability analysis

Theorem 1. *With the projection type adaptation law Eq. (36), the proposed control law Eq. (31) guarantees that:*

A. The tracking error can be always bounded by

$$|e_1|\leqslant\sqrt{2\exp(-\lambda t)V_1(0)+\frac{2\varepsilon}{\lambda}(1-\exp(-\lambda t))} \tag{37}$$

where $\lambda=2k_1$ is the exponentially converging rate.

B. If use a sufficient number of fuzzy rules, the minimum approximation errors w_g and w_h can approach zero based on the universal approximation theorem.[17] In this case, in addition to results in A, asymptotic input tracking is also achieved, i.e. $e_1\to0$ as $t\to\infty$.

Proof. Noting Eqs. (31)–(33), the time derivative of V_1 satisfies:

$$\dot{V}_1\leqslant e_1\alpha Q_{Lr1}+\varepsilon\leqslant-k_1e_1^2+\varepsilon=-2k_1V_1+\varepsilon \tag{38}$$

Therefore, we can obtain

$$V_1(t)\leqslant\exp(-\lambda t)V_1(0)+\frac{\varepsilon}{\lambda}(1-\exp(-\lambda t)) \tag{39}$$

From Eq. (39) and noting the definition of V_1 in Eq. (17), the tracking error can be always bounded by

$$|e_1|\leqslant\sqrt{2\exp(-\lambda t)V_1(0)+\frac{2\varepsilon}{\lambda}(1-\exp(-\lambda t))} \tag{40}$$

Then the tracking error e_1 is bounded. Now consider the situation in B of Theorem 1. Choose a Lyapunov function candidate be

$$V_s=V_1+\frac{1}{2\gamma_1}\tilde{\boldsymbol{\Theta}}_g^\mathrm{T}\tilde{\boldsymbol{\Theta}}_g+\frac{1}{2\gamma_2}\tilde{\boldsymbol{\Theta}}_h^\mathrm{T}\tilde{\boldsymbol{\Theta}}_h \tag{41}$$

where $\gamma_1>0$, $\gamma_2>0$, $\tilde{\boldsymbol{\Theta}}_g=\boldsymbol{\Theta}_g^*-\boldsymbol{\Theta}_g$ and $\tilde{\boldsymbol{\Theta}}_h=\boldsymbol{\Theta}_h^*-\boldsymbol{\Theta}_h$.

Differentiating V_s with respect to time yields

$$\begin{aligned}\dot{V}_s=\dot{V}_1&+\frac{1}{\gamma_1}\tilde{\boldsymbol{\Theta}}_g^\mathrm{T}\dot{\boldsymbol{\Theta}}_g+\frac{1}{\gamma_2}\tilde{\boldsymbol{\Theta}}_h^\mathrm{T}\dot{\boldsymbol{\Theta}}_h=e_1(\alpha Q_\mathrm{Lr}-\tilde{\boldsymbol{\Theta}}_g^\mathrm{T}\boldsymbol{\xi}_g(P_\mathrm{L},x_1)\\&-\tilde{\boldsymbol{\Theta}}_h^\mathrm{T}\boldsymbol{\xi}_h(\dot{P}_\mathrm{L},x_1))+\frac{1}{\gamma_1}\tilde{\boldsymbol{\Theta}}_g^\mathrm{T}\dot{\boldsymbol{\Theta}}_g+\frac{1}{\gamma_2}\tilde{\boldsymbol{\Theta}}_h^\mathrm{T}\dot{\boldsymbol{\Theta}}_h=\alpha e_1Q_\mathrm{Lr}\\&+\tilde{\boldsymbol{\Theta}}_g^\mathrm{T}\left(\frac{1}{\gamma_1}\dot{\boldsymbol{\Theta}}_g-e_1\boldsymbol{\xi}_g(P_L,x_1)\right)+\tilde{\boldsymbol{\Theta}}_h^\mathrm{T}\left(\frac{1}{\gamma_2}\dot{\boldsymbol{\Theta}}_h-e_1\boldsymbol{\xi}_h(\dot{P}_\mathrm{L},x_1)\right)\end{aligned} \tag{42}$$

Noting the projection type adaptation law and the property of Eq. (34), then

$$\begin{aligned}\dot{V}_s&=\alpha e_1Q_\mathrm{Lr}+\tilde{\boldsymbol{\Theta}}_g^\mathrm{T}\left(\frac{1}{\gamma_1}\mathrm{Proj}_{\boldsymbol{\Theta}_g}(\gamma_1\boldsymbol{\tau}_g)-e_1\boldsymbol{\xi}_g(P_\mathrm{L},x_1)\right)\\&\quad+\tilde{\boldsymbol{\Theta}}_h^\mathrm{T}\left(\frac{1}{\gamma_2}\mathrm{Proj}_{\boldsymbol{\Theta}_h}(\gamma_2\boldsymbol{\tau}_h)-e_1\boldsymbol{\xi}_h(\dot{P}_\mathrm{L},x_1)\right)\\&\leqslant-ke_1^2\triangleq-W\end{aligned} \tag{43}$$

That is to say, $V_s\leqslant V_s(0)$. Therefore, $W\in L_2$ and $V_s\in L_\infty$. Since e_1 are bounded, it is easy to check that $\dot{W}$ is bounded and thus uniformly continuous. By Barbalat's lemma, $W\to0$ as $t\to\infty$, which lead to B of Theorem 1. □

So the next step is to get the real control input u from the desired flow Q_L. With Eq. (8), the main difficult is how to determine the accurate values of C_d and ω. Fortunately, it is easy to know the rated flow at certain valve pressure drop ΔP_{drop} in general. For example, all the servo valves of Moog company will give the rated flow Q_{rated} through the valve at certain pressure drop $\Delta P_{\mathrm{drop}}=7$ MPa.

$$Q_{\mathrm{rated}}=C_\mathrm{d}\omega u_{\max}\sqrt{\Delta P_{\mathrm{drop}}/\rho} \tag{44}$$

where $u_{\max}$ is the saturated input of servo valve and Q_{rated} the rated flow when the pressure drop is ΔP_{drop}.

Combining Eqs. (8) and (44), the real control input can be synthesized as

$$u=\frac{Q_\mathrm{L}}{Q_{\mathrm{rated}}}\sqrt{\frac{\Delta P_{\mathrm{drop}}}{P_s-\mathrm{sgn}(u)P_\mathrm{L}}}\cdot u_{\max}=\frac{Q_\mathrm{L}}{R(u,P_\mathrm{L})} \tag{45}$$

where the flow gain

$$R(u,P_L)=\frac{Q_{\mathrm{rated}}}{u_{\max}}\sqrt{\frac{P_s-\mathrm{sgn}(u)P_\mathrm{L}}{\Delta P_{\mathrm{drop}}}}.$$

4. Experiment verification

4.1. Experimental setup configuration

Comparative experiments are performed on the test platform, shown in Fig. 2. It consists of five parts: hydraulic power supply, Moog servo-valve, hydraulic motor, angle encoder and control cabinet. The key experimental parameters are listed in Table 1. The entire system is controlled by real-time control program based on RTX real-time operating system and Labwindows/CVI, and the control period time is 1 ms.

4.2. Comparative experiments

Define five fuzzy sets with labels, namely, negative big (NB), negative small (NS), zero (ZO), positive small (PS) and positive big (PB). The Gaussian membership functions are defined as

$$\mu_{A^k}(x)=\exp\left\{-\left[\left(x+\frac{(k-2)x_{\max}}{2}\right)\Big/\frac{x_{\max}}{4}\right]^2\right\}\quad(k=0,1,2,3,4) \tag{46}$$

where A^k refers to NB, NS, ZO, PS and PB when $k=0$, 1, 2, 3, 4; x and $x_{\max}$ represent input variable and the upper bound of input variable. Load pressure P_L and its derivative $\dot{P}_\mathrm{L}$ required in the control law are filtered by fourth-order butterworth filters with 200 Hz and 100 Hz cut-off frequencies, respectively. In order to eliminate the chattering caused by the sign function in Eq. (45), the sign function is replaced by a smooth hyperbolic function during the experiment.

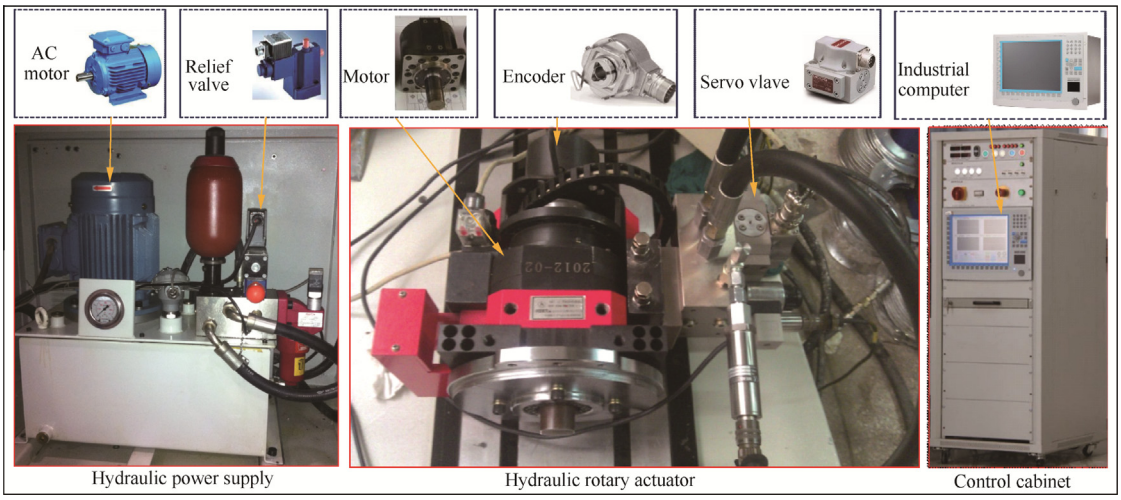

Fig. 2 Test platform.

Table 1 Key experimental parameters of test system.

Component	Specification	Mark
Hydraulic motor	D_L: 7 cm^3/rad, Range: ±35° Payload: 0.05 kg m^2	Self-development
Servo valve	G761–3002	MOOG
Digital encoder	ECN413	HEIDENHAIN
Industrial computer	IEI WS-855GS	ADVANTECH
A/D card	PCI-1716/16	ADVANTECH
D/A card	PCI-1723/8, 16 bit DAC	ADVANTECH
Encode card	IK220	HEIDENHAIN
Pump	GHP1A-D-7	MARZOCCHI
AC motor	M2QA, 3 kW, 280 V	ABB
Relief valve	DBEE6–1X/200G24K31 M	REXROTH

The parameters of nonlinear fuzzy robust controller (NFRC) based on Eq. (38) are $k_1 + k_s = 50$, $\theta_{10} = 4.77 \times 10^{-8}$, $\theta_{20} = 1.372 \times 10^{-9}$, $\gamma_g = 3000$, $\gamma_h = 3000$, $P_s = 8 \times 10^6$, $\alpha = 1.43 \times 10^5$. The upper bounds of P_L, x_1 and $\dot{P}_L$ are 3×10^6 Pa, 20° and 3.5×10^8 Pa/s, respectively. The desired trajectories are given as $x_{1d} = 5(1 - \exp(-t))(1 - \cos(12.56t))$.

The experimental results of the proposed NFRC controller are shown in Fig. 3. As illustrated in Fig. 3, tracking errors converge from 0.37° to 0.07°.

In order to analyze the effect of fuzzy compensators, the compensating control $\frac{\hat{g}(P_L, x_1|\boldsymbol{\Theta}_g)}{\alpha R(u, P_L)}$ and $\frac{\hat{h}(\dot{P}_L, x_1|\boldsymbol{\Theta}_h)}{\alpha R(u, P_L)}$, corresponding to $\hat{g}$ and $\hat{h}$, are illustrated in Fig. 4. It is obvious that the fuzzy estimation of model uncertainties can achieve stable state.

Three algorithms will be compared to verify the effectiveness of the proposed control scheme.

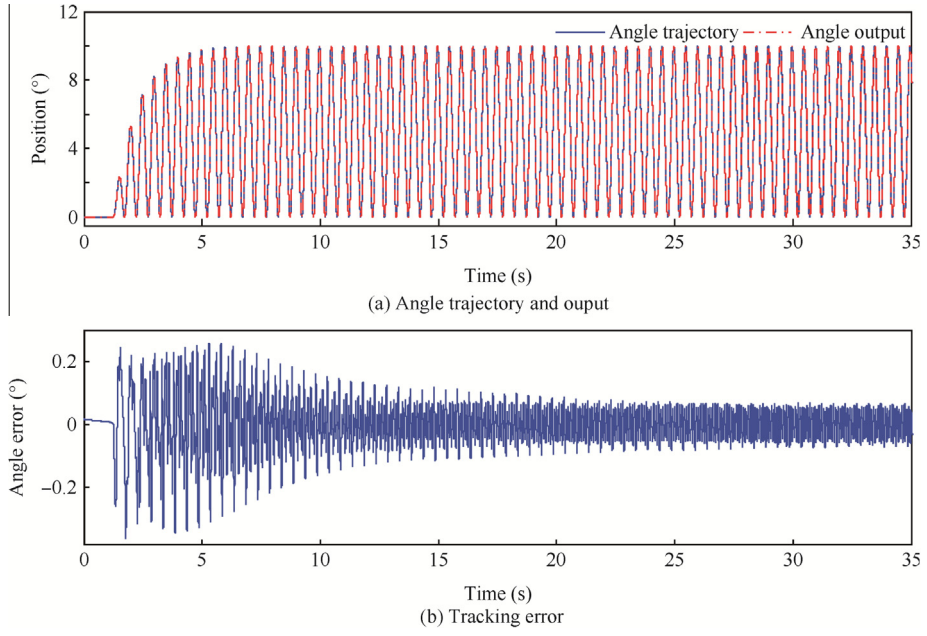

Fig. 3 Angle tracking performance of NFRC.

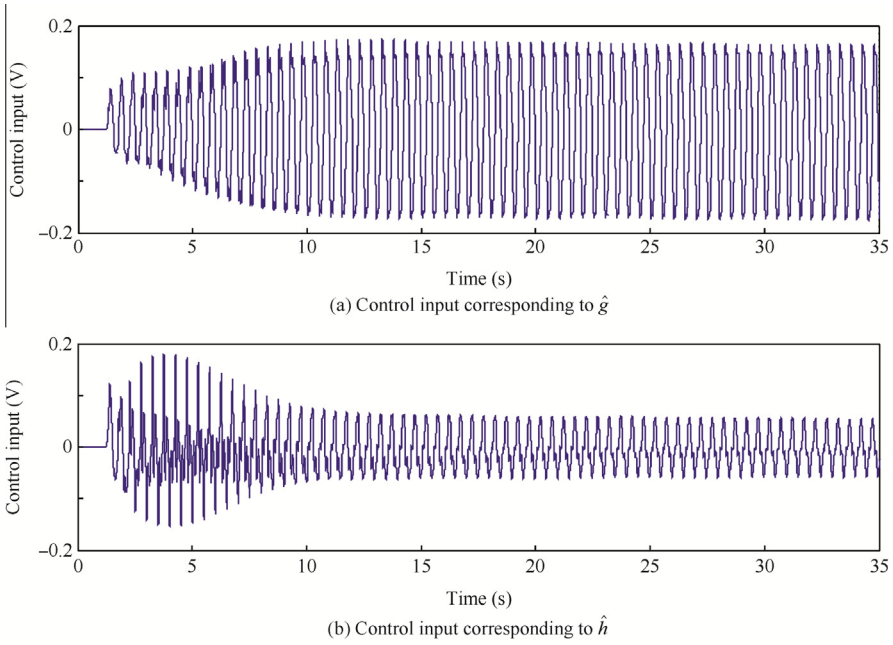

Fig. 4 Controller input of fuzzy compensators.

(1) NFRC: nonlinear fuzzy robust controller based on the proposed control law Eq. (31) and the projection type adaptation law Eq. (28).
(2) Nonlinear robust controller (NRC). The control law is given by

$$\begin{cases} Q_{\mathrm{L}} = Q_{\mathrm{La}} + Q_{\mathrm{Lr1}} + Q_{\mathrm{Lr2}} \\ Q_{\mathrm{La}} = \frac{1}{\alpha}(\dot{x}_{1d} + \theta_{10}\dot{P}_{\mathrm{L}} + \theta_{20}P_{\mathrm{L}}) \\ Q_{\mathrm{Lr1}} = -k_1 e_1/\alpha \\ Q_{\mathrm{Lr2}} = -\frac{1}{\alpha}k_{\mathrm{s}}(P_{\mathrm{L}}, \dot{P}_{\mathrm{L}}, x_1)e_1 \end{cases} \tag{47}$$

Make the robust term Q_{Lr2} be any function satisfying the following conditions:

Condition 1.

$$e_1(\alpha Q_{\mathrm{Lr2}} - \tilde{\boldsymbol{\theta}}^{\mathrm{T}}\boldsymbol{\varphi} + d_{\mathrm{L}}) \leqslant \varepsilon \tag{48}$$

Condition 2.

$$\alpha e_1 Q_{\mathrm{Lr2}} \leqslant 0 \tag{49}$$

(1) Traditional robust controller (RC&V) based on angle-errors with velocity $\dot{x}_{1\mathrm{d}}$ feed-forward compensation. The control law is given by

$$\begin{cases} Q_{\mathrm{L}} = Q_{\mathrm{La}} + Q_{\mathrm{Lr1}} + Q_{\mathrm{Lr2}} \\ Q_{\mathrm{La}} = \frac{1}{\alpha}\dot{x}_{1\mathrm{d}} \\ Q_{\mathrm{Lr1}} = -k_1 e_1/\alpha \\ Q_{\mathrm{Lr2}} = -\frac{1}{\alpha}k_{\mathrm{s}}(P_{\mathrm{L}}, \dot{P}_{\mathrm{L}}, x_1)e_1 \end{cases} \tag{50}$$

Make the robust term Q_{Lr2} be any function satisfying the following conditions:

Condition 1.

$$e_1(\alpha Q_{\mathrm{Lr2}} - \boldsymbol{\theta}^{\mathrm{T}}\boldsymbol{\varphi} + d_{\mathrm{L}}) \leqslant \varepsilon \tag{51}$$

Condition 2.

$$\alpha e_1 Q_{\mathrm{Lr2}} \leqslant 0 \tag{52}$$

In the above three controllers, we can choose the needed robust control gains $k_{\mathrm{s}}(P_{\mathrm{L}}, \dot{P}_{\mathrm{L}}, x_1)$ in the following two ways. The first method is to calculate $k_{\mathrm{s}}(P_{\mathrm{L}}, \dot{P}_{\mathrm{L}}, x_1)$ rigorously online to satisfy the conditions Eqs. (33) and (34), Eqs. (48) and (49) and Eqs. (51) and (52) respectively. However, it increases the complexity of the control law considerably since it may need significant amount of investigating work and computation time, sometimes even be impossible. Alternatively, a pragmatic approach is to simply choose $k_{\mathrm{s}}(P_{\mathrm{L}}, \dot{P}_{\mathrm{L}}, x_1)$ large enough without worrying about the specific prerequisites. In this way, the conditions Eqs. (33) and (34), Eqs. (48) and (49) and Eqs. (51) and (52) will be satisfied for a certain set of values of $k_{\mathrm{s}}(P_{\mathrm{L}}, \dot{P}_{\mathrm{L}}, x_1)$ at least locally around the desired trajectory to be tracked.[3,32,34] In this paper, the second approach is used since it facilitates the online tuning process of gains in implementation. In order to ensure a fair comparison, the above three controllers have the same robust control gains.

Then angle trajectory and stable tracking errors under the above three control laws are shown in Fig. 5. The results show that the maximum tracking errors are 0.07°, 0.46° and 0.71°, respectively. It shows that compared with the RC&V, the performances based on the NRC controller and the proposed NFRC controller are improved by 35.2% and 90.1%, respectively. The tracking errors of NFRC and NRC are smaller than that of RC&V due to the model-based compensation of P_{L} and $\dot{P}_{\mathrm{L}}$. NFRC is much more effective

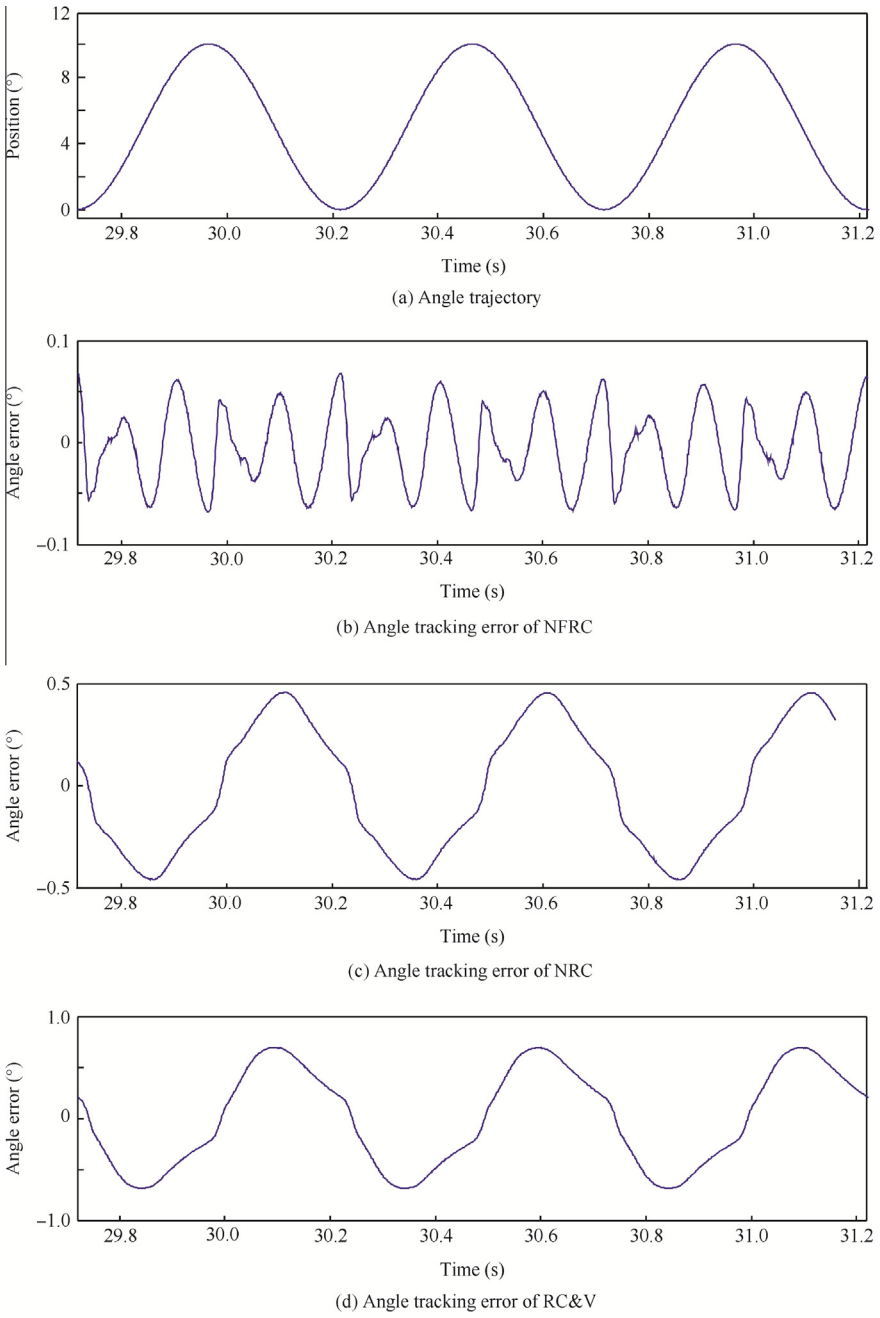

Fig. 5 Angle trajectory and comparative tracking errors.

than NRC due to fuzzy compensators of parameter uncertainty and nonlinear uncertainty for Q_{Leakage} and Q_{Elastic}. It is obvious that the proposed NFRC can effectively overcome structured and unstructured uncertainties to obtain the best tracking accuracy.

To further analyze the effect of fuzzy compensator about Q_{Leakage}, the controller input $\frac{\hat{g}(P_{\text{L}},x_1|\boldsymbol{\Theta}_{\hat{g}})}{\alpha R(u,P_{\text{L}})}$ corresponding to $\hat{g}$ and load pressure P_{L} are shown in Fig. 6. It can be found that the stable estimation of leakage flow $\hat{g}$ has the similar change rule to P_{L}.

To further analyze the effect of fuzzy compensator about Q_{Elastic}, the controller inputs $\frac{\hat{h}(\dot{P}_{\text{L}},x_1|\boldsymbol{\Theta}_{\hat{h}})}{\alpha R(u,P_{\text{L}})}$ corresponding to $\hat{h}$ and $\dot{P}_{\text{L}}$ are shown in Fig. 7. It can be found that the stable estimation of leakage flow $\hat{h}$ has the similar change rule to $\dot{P}_{\text{L}}$. The total control input of NFRC is shown in Fig. 8. The control input is also very smooth.

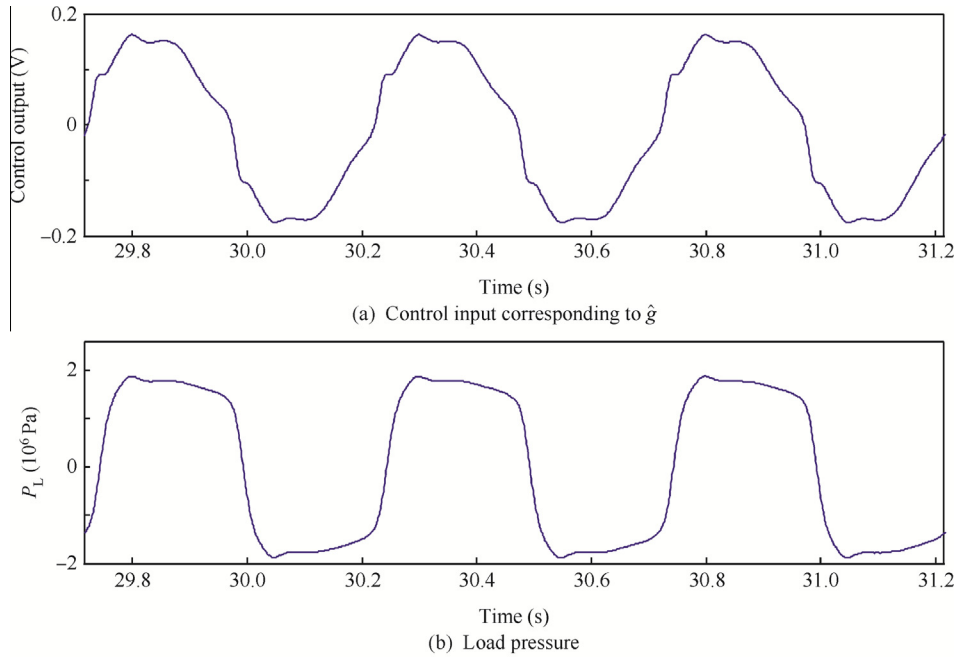

Fig. 6 Comparison of $\hat{g}$ and P_L.

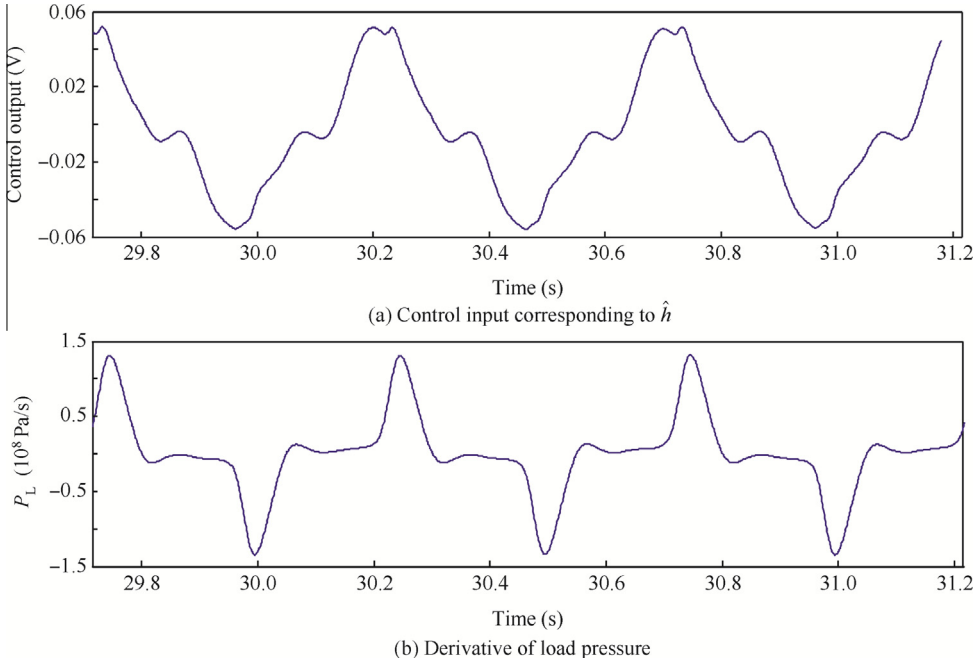

Fig. 7 Comparison of $\hat{h}$ and P_L.

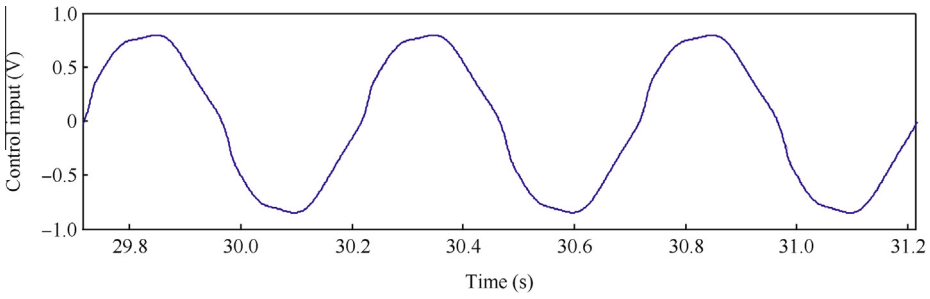

Fig. 8 Total control input of NFRC.

5. Conclusions

In this paper, a practical nonlinear fuzzy robust cont-roller is developed for hydraulic rotary actuators in HFMS. Comparative experiment results show that adaptive fuzzy compensators can effectively deal with parametric uncertainty and unstructured uncertainties from Q_{Leakage} and Q_{Elastic} in hydraulic rotary actuators. Meanwhile, the proposed controller can achieve a guaranteed transient performance and better final tracking accuracy.

Acknowledgements

This work was supported by the National Basic Research Program of China (No. 2014CB046406) and the National Natural Science Foundation of China (No. 51235002)

References

1. Guo ZF, Cao J, Zhao KD. Design and experiments of model-free compound controller of flight simulator. *Chin J Aeronaut* 2009; **22**(6):644–8.
2. Wang BY, Dong YL, Zhao KD. Compound control for hydraulic flight motion simulator. *Chin J Aeronaut* 2010;**23**(2):240–5.
3. Yao JY, Jiao ZX, Han SS. Friction compensation for low velocity control of hydraulic flight motion simulator: a simple adaptive robust approach. *Chin J Aeronaut* 2013;**26**(3):814–22.
4. Kim W, Won D, Chung CC. High gain observer based nonlinear position control for electro hydraulic servo systems. *Proceedings of American control conference*. Baltimore, MD. Piscataway, NJ: IEEE; 2010. p. 1440–6, Jun 30–Jul 2.
5. Merritt HE. *Hydraulic control systems*. New York: John Wiley &Sons; 1967. p. 148.
6. Yao B, Bu FP, Chiu GTC. Nonlinear adaptive robust control of electro-hydraulic servo systems with discontinuous projections. *Proceedings of the 37th IEEE conference on decision and control*. Tampa, Florida. Piscataway, NJ: IEEE; 1998. p. 2265–70, Dec 16–18.
7. Tsao TC, Tomizuka M. Robust adaptive and repetitive digital Tracking control and application to a hydraulic servo for noncircular machining. *J Dynam Syst, Measur, Control* 1994;**116**(1):624–32.
8. Wang CW, Jiao ZX, Wu S, Shang YX. An experimental study of the dual-loop control of electro-hydraulic load simulator. *Chin J Aeronaut* 2013;**26**(6):1586–95.
9. Han SS, Jiao ZX, Yao JY, Shang YX. Compound velocity synchronizing control strategy for electro-hydraulic load simulator and its engineering application. *J Dynam Syst, Measur, Control* 2014;**136**(5):0510021–5100213.
10. Vossoughi R, Donath M. Dynamic feedback linearization for electro-hydraulically actuated control systems. *J Dynam Syst, Measur, Control* 1995;**117**(4):468–77.
11. Alleyne A, Hedrick JK. Nonlinear adaptive control of active suspension. *IEEE Trans Control Syst Technol* 1995;**3**(1):94–101.
12. Yue X, Vilathgamuwa DM, Tseng KJ. Robust adaptive control of a three-axis motion simulator with state observers. *IEEE-ASME Trans Mechatron* 2005;**10**(4):437–48.
13. Yao B, Bu FP, Reedy J, Chiu G. Adaptive robust control of single-rod hydraulic actuators: theory and experiments. *IEEE-ASME Trans Mechatron* 2000;**5**(1):79–91.
14. Mohanty A, Yao B. Indirect adaptive robust control of hydraulic manipulators with accurate parameter estimates. *IEEE Trans Control Syst Technol* 2011;**19**(3):567–75.
15. Mohanty A, Yao B. Integrated direct/indirect adaptive robust control of hydraulic manipulators with valve deadband. *IEEE-ASME Trans Mechatron* 2011;**16**(4):707–15.
16. Mohanty A. Some generalization to the theory of adaptive robust control and its applciation [dissertation]. Lafayette: Purdue University; 2010.
17. Wang LX. Fuzzy systems are universal approximators. *Proceedings of IEEE international conference on fuzzy systems*. San Diego, CA. Piscataway, NJ: IEEE; 1992. p. 1163–70, Mar 8–12.
18. Wang LX. Stable adaptive fuzzy control of nonlinear systems. *Proceedings of the 31st IEEE conference on decision and control*. Tucson, AZ. Piscataway, NJ: IEEE; 1992. p. 2511–6, Dec 16–18.
19. Shao JP, Chen LH, Sun ZB. The application of fuzzy control strategy in electro-hydraulic servo system. *Proceedings of the IEEE international conference on mechatronics and automation*. Niagara Falls, Canada. Piscataway, NJ: IEEE; 2005. p. 2010–6, Jul 29–Aug 1.
20. Park J, Sandberg IW. Universal approximation using radial basis-function network. *Neural Comput* 1991;**3**(2):246–57.
21. Hornik K. Approximation capabilities of multiplayer feed-forward networks. *Neural Netw* 1991;**4**(2):251–7.
22. Chen CQ, Tang HJ, Qi SS, Cheng Y, Feng HS, Peng XB, et al. An electro-hydraulic servo control system research for CFETR blanket RH. *Fusion Eng Design* 2014;**89**(11):2806–13.
23. Pedro JO, Dangor M, Dahunsi OA. Montaz Ali M. Intelligent feedback linearization control of nonlinear electrohydraulic suspension systems using particle swarm optimization. *Appl Soft Comput* 2014;**24**:50–62.
24. Branco PJC, Dente JA. Control of an electro-hydraulic system using neuro-fuzzy modelling and real-time learning approaches. *Knowl-based Syst* 1997;**1**(4):190–206.
25. Jiang ZM, Wang SW, Lin TQ. Variable structure control of electro-hydraulic servo systems using fuzzy CMAC neural network. *Trans Inst Measur Control* 2003;**25**(3):185–201.
26. Liu YF, Miao D. Research on adaptive fuzzy sliding mode control for electro-hydraulic servo system. *Proc CSEE* 2006;**26**(14):140–4 Chinese.
27. Zhang JT, Cheng DF, Liu YF, Zhu GL. Adaptive fuzzy sliding mode control for missile electro-hydraulic servo mechanism. *Proceedings of the 7th world congress on intelligent control and automation*. Chongqing. Piscataway, NJ: IEEE; 2008. p. 5197–202, Jun 25–27.
28. Ran MP, Wang Q, Hou DL, Dong CY. Backstepping design of missile guidance and control based on adaptive fuzzy sliding mode control. *Chin J Aeronaut* 2014;**27**(3):634–42.
29. Wang XJ, Wang SP, Zhao P. Adaptive fuzzy torque control of passive torque servo systems based on small gain theorem and input-to-state stability. *Chin J Aeronaut* 2012;**25**(6):906–16.
30. Yoo BK, Ham WC. Adaptive control of robot manipulator using fuzzy compensator. *IEEE Trans Fuzzy Syst* 2000;**8**(2):212–6.
31. Nikas GK, Burridge G, Sayles RS. Modelling and optimization of rotary vane seals. *J Eng Tribol* 2007;**221**(6):699–715.
32. Yao JY, Jiao ZX, Ma DW, Yan L. High-accuracy tracking control of hydraulic rotary actuators with modeling uncertainties. *IEEE-ASME Trans Mechatron* 2014;**19**(2):633–41.
33. Guan C, Pan SX. Adaptive sliding mode control of electro-hydraulic system with nonlinear unknown parameters. *Control Eng Pract* 2008;**16**(11):1275–84.
34. Yao JY, Jiao ZX, Yao B, Shang YX, Dong WB. Nonlinear adaptive robust force control of hydraulic load simulator. *Chin J Aeronaut* 2012;**25**(5):766–75.

Han Songshan is a Ph.D. student in Beihang University. His main research interests include hydraulic servo control, modeling and simulation, dynamics and control of mechatronic systems.

Jiao Zongxia is a professor and Ph.D. advisor in Beihang University. He received his Ph.D. degree from Zhejiang University in 1991. His current research interests are fluid power transmission and control, mechatronics systems and simulation engineering.